Journal of Physics B: Atomic, Molecular and Optical Physics

PAPER • **OPEN ACCESS**

Spectral broadening for pulse compression using liquid alcohols

To cite this article: Jacob A Stephen *et al* 2022 *J. Phys. B: At. Mol. Opt. Phys.* **55** 155402

OPEN ACCESS
IOP Publishing
Journal of Physics B: Atomic, Molecular and Optical Physics
J. Phys. B: At. Mol. Opt. Phys. **55** (2022) 155402 (7pp)
https://doi.org/10.1088/1361-6455/ac7990

Spectral broadening for pulse compression using liquid alcohols

Jacob A Stephen*, Chathurangani Jayalath Arachchige and T J Hammond

Department of Physics, University of Windsor, 401 Sunset Dr., Windsor, ON N9B 3P4, Canada

E-mail: stephenh@uwindsor.ca

Received 28 February 2022, revised 26 May 2022
Accepted for publication 15 June 2022
Published 4 July 2022

Abstract

Although gases, and more recently solids, have been used to create few-cycle pulses, we explore using liquid alcohols for spectral broadening and femtosecond pulse compression. By using a series of 1 cm cuvettes filled with 1-decanol, we have compressed a pulse from 83.6 fs down to 31.3 fs with a spectrum capable of supporting 25 fs pulses without filamentation. We measure the nonlinear index of refraction for various liquids, measuring $n_2 = (6.8 \pm 0.5) \times 10^{-20}$ m^2 W^{-1} for 1-decanol. We demonstrate liquids to be a compact, simple, versatile, and cost-effective material to obtain broad spectra.

Keywords: spectral, broadening, pulse, compressions, liquid, alcohols, ultrafast

(Some figures may appear in colour only in the online journal)

1. Introduction

Ultrafast photonics is a branch of optics that deals with ultrashort laser pulses on the order of femtoseconds (1 fs = 10^{-15} s); prominent experiments within this field explore ultrashort laser pulses to observe light–matter interactions and phenomena on time scales of picoseconds (1 ps = 10^{-12} s) or shorter. Ultrashort laser pulses also play a large role in measuring the nonlinear response of materials to high intensity pulses. Ultrafast technologies have been used in a wide variety of applications, including pulse compression techniques for few-cycles pulses via self-phase modulation (SPM) [1–3], Kerr instability amplification [4, 5], and generation of ultrashort pulses in the infrared (IR) and terahertz (THz) regimes [6–8]. Femtosecond pulse durations also allow for the investigation of processes that occur on femtosecond to attosecond (1 as = 10^{-18} s) time scales, such as high harmonic generation [9, 10] and femtosecond [11, 12] and attosecond pump–probe experiments [13].

Laser amplifiers and oscillators can support broad spectra that create ultrashort pulses, however, even gain media that can support the broadest bandwidths, such as Ti:sapphire and ytterbium-doped lasers, suffer from gain-narrowing that limits the spectral bandwidth. The impetus for shorter pulses will always lead to bandwidths that cannot be supported by the gain medium [14, 15]. Ultrashort pulses can be created by increasing the spectral bandwidth of a pulse through SPM and subsequently compensating the phase induced in SPM by group-delay dispersion (GDD).

Pulse compression experiments can be performed using a variety of methods to achieve spectral broadening such as all-solid state relays [16–20], gas-filled hollow-core fibres (HCF) [21–25], solid-core fibres [26, 27], multi-pass cells [28, 29], and single-pass bulk materials [30]. Solid-state pulse compression schemes boast higher transmission rates than gas and HCF setups but output lower energy pulses, typically from 1–100 μJ [17]. Solid-state setups are more susceptible to self-focusing than gases, which can cause damage to the material. The critical power for self-focusing in a solid is on the order of a few MW, whereas in a gas, it is ∼10 GW [16]. Single-pass solid-state setups typically provide lower compression factors than single-pass gas-filled HCF setups, however those compression factors can be increased with multi-pass configurations.

* Author to whom any correspondence should be addressed.

Multi-pass configurations allow for higher compression factors at the cost of higher loss by lowering transmission [21], while broadening the spectrum more than a single pass would [31]. Gas-filled HCFs require a large amount of space to set up, typically using fibres of a few metres in length, and require vacuum chambers to isolate the gas [21, 22], whereas a solid-state setup requires much less space and can be easier to construct and maintain [17]. In this work, we investigate using liquids for spectral broadening in pulse compression experiments, in order to bypass the disadvantages of using solids or gases.

Supercontinuum generation has been observed in water [32], indicating that liquids can provide a suitable alternative to solids and gases in pulse compression experiments. We propose the use of liquid alcohols, namely 1-decanol, for spectral broadening and pulse compression. Liquids are much easier to set up and manage, and do not run the risk of permanently damaging under high intensities as a liquid remains functionally stable once damaged. Liquids can also be cheaper and easier to obtain; if a material needs to be exchanged for another, one can simply empty and refill the container holding the liquid and continue the experiment. We organize this paper in the following manner: we characterize the nonlinear index of refraction (n_2) of several liquids using a 100 fs laser in a Z-scan measurement, we determine the spectral broadening due to SPM in 1-decanol, and we measure the resulting compressed pulse using frequency resolved optical gating (FROG).

2. Measuring the nonlinear index of refraction of decanol using the Z-scan method

In order to measure the n_2 of 1-decanol, we perform a closed-aperture Z-scan [33]. We perform the experiments using a 780 nm Ti:sapphire laser with a beam waist ($1/e^2$ radius) of 2.5 mm. Our laser operates with a repetition rate of 1 kHz and produces 83.6 fs pulses with an energy of 1 mJ. We place a 1 cm quartz cuvette (the dimensions of the cuvette are 1.2 × 1.1 cm; each quartz wall is 0.1 cm thick, providing 1.0 cm of liquid for the beam to travel through) filled with decanol on a motorized translation stage and pass the sample through the focus generated by a lens with a focal length of 200 mm. Figure 1 shows the Z-scan setup.

The stage travels 25 mm, measuring the power transmitted through the aperture every 0.25 mm. A half-wave plate is used in conjunction with a wire-grid polarizer to control the power entering the apparatus. A 50/50 beam splitter is placed before the lens to pick off half of the beam in order to measure any potential fluctuations in the output power.

The data is fitted to the function [34]

$$T = 1 + \Delta\Phi F(\zeta, l) \tag{1}$$

using a least squares fit, where $\Delta\Phi = (2\pi/\lambda)n_2 z_0 I_0$ is the phase shift induced by self-focusing; λ and I_0 are the wavelength and intensity of the pulse respectively and z_0 is the Rayleigh range. The distinctive Z-scan curve comes from $F(\zeta, l)$, a function of normalized lengths, $\zeta = z/z_0$ and $l = L/z_0$, where z is the direction in which the beam is propagating and L is the thickness of the sample that is being probed.

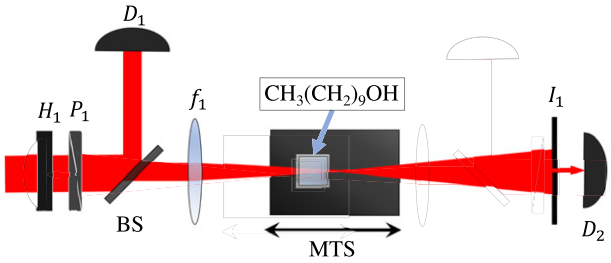

Figure 1. Diagram of Z-scan setup used to determine n_2 of decanol. In this diagram, the beam is travelling left to right. D_N, I_1, f_1, P_1, H_1, MTS, and BS are the power detectors, clipping iris, 200 mm focal length lens, wire-grid polarizer, half-wave plate, motorized translation stage, and 50/50 beam splitter, respectively.

We define $F(\zeta, l)$ as [34]

$$F(\zeta, l) = \frac{1}{4}\ln\left(\frac{\left[(\zeta + l/2)^2 + 1\right]\left[(\zeta - l/2)^2 + 9\right]}{\left[(\zeta - l/2)^2 + 1\right]\left[(\zeta + l/2)^2 + 9\right]}\right). \tag{2}$$

By extracting $\Delta\Phi$ from the least-squares fit, we can determine the n_2 of the material. We perform ten scans on each material, averaging the n_2 values extracted from each scan. The uncertainty associated with n_2 comes from the standard deviation of the ten runs taken. A sample scan performed on decanol can be seen in figure 2. In addition to measuring the n_2 of decanol, we also measure the n_2 of several other materials for which the n_2 may or may not have been previously reported, namely 1-pentanol, water, and sapphire. The results of our Z-scan measurements can be seen in table 1.

3. Spectral broadening using decanol

In order to compress the pulse, we first seek to broaden the spectrum using 1-decanol. To achieve this spectral broadening, we exploit SPM to induce a phase shift:

$$\Delta\phi_{\mathrm{SPM}} = -\frac{n_2\omega_0 L}{c} I_0, \tag{3}$$

where c is the speed of light in vacuum and ω_0 is the frequency of the pulse. We can roughly define a compression factor, K_c, as the ratio of the spectral bandwidths before and after the SPM:

$$K_c = \frac{\Delta\omega_{\mathrm{out}}}{\Delta\omega_{\mathrm{in}}}. \tag{4}$$

By broadening the spectrum, we can increase this compression factor.

To broaden the spectrum, we begin with methanol, due to its relatively large n_2 (6.7×10^{-20} W m^{-2}) [35]. We find that the beam shape becomes highly distorted upon propagation through methanol due to the type of filament that is being generated. The filament that we observe in liquid differs from that generated in air, where the generated plasma has an index of refraction less than unity [38]. This type of filament in a liquid can be created by thermal lensing [39] or boiling the liquid. Higher intensities will cause a liquid to increase in temperature, leading to a change in the index of refraction. This change in the index of refraction (n) with temperature (T), dn/dT, can

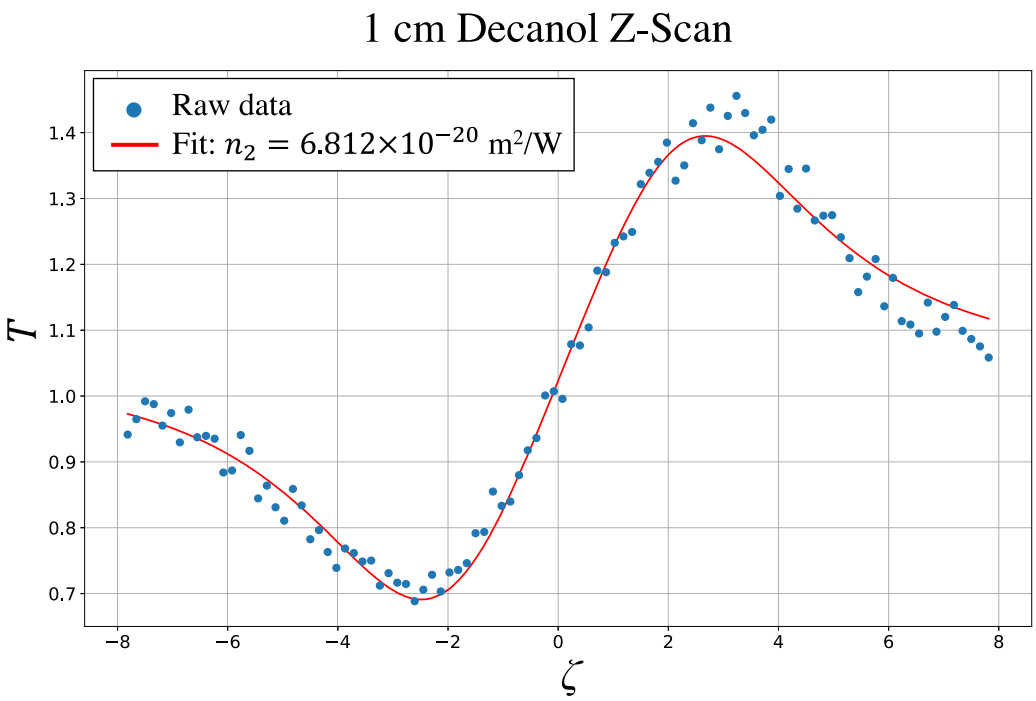

Figure 2. Data obtained from a single Z-scan of 1 cm of 1-decanol. The data is plotted as the transmittance (T) against ζ. The blue dots show the raw data while the red curve is the nonlinear least squares fit of the function from equation (1). We report the average of ten scans.

Table 1. Nonlinear indices of refraction measured using the Z-scan technique. All values of n_2 are measured with a pulse duration of 83.6 fs at a wavelength of 780 nm. The values we measure are compared to n_2 values found in other literature sources. To the best of our knowledge, there are no recorded values for n_2 of 1-pentanol. ∗No value for uncertainty reported in literature.

Material	n_2 measured ($\times10^{-20}$ m^2 W^{-1})	n_2 from literature ($\times10^{-20}$ m^2 W^{-1})	Method used in literature	Wavelength used in literature	Pulse duration used in literature
Water	5.5 ± 0.3	5.7 ± 0.5 [35]	ENSTA-method	804 nm	150 fs
Sapphire	2.0 ± 0.1	2.8 ± 0.8 [36]	Z-scan	1550 nm	1 ps
Pentanol	7.0 ± 0.4	NR	NR	NR	NR
Decanol	6.8 ± 0.5	11∗ [37]	Optical Kerr gate	1.06 μm	10 ps

generate a thermal lens which can cause filamentation [40]. Studies have shown that the index of refraction of all alcohol chains from n-methanol to n-decanol change as a function of temperature at the same rate, $\mathrm{d}n/\mathrm{d}T = 4 \times 10^{-4}\,^{\circ}\mathrm{C}^{-1}$ [41]. For materials in which $\mathrm{d}n/\mathrm{d}T$ is the same, the materials in question should create a thermal lens at the same rate, if they are not damaged or boiled.

The low boiling point of methanol (64.7 °C [42]) will cause the liquid to boil at low intensities, leading to thermal effects [43, 44] that change the density of the liquid, creating this filament. Decanol has a higher boiling point than methanol (229 °C [45]), though we do not observe any filamentation within decanol given our conditions presented here. Since we do not see decanol filament at the same intensity that we see methanol filament, we infer that the boiling of the liquid is generating a filament, not a thermal lens.

To test this hypothesis we investigate alcohols of higher boiling points, such as pentanol and decanol. In those cases, we find that the boiling points of alcohols increase with number of carbon constituents in the carbon chain, whereas the ionization potential decreases with each added carbon atom (figure 3). Plasma filamentation is dependent on ionization energy, whereas thermal lensing is dependent on the temperature of the material. The trends in these chemical properties indicate that larger alcohols are easier to ionize, but will not create a thermal lens at as low an intensity as a smaller alcohol.

We opt to use 1-pentanol (pentanol) and 1-decanol (decanol), due to their high boiling points, to avoid thermal effects that may distort the beam profile while looking to maintain similar optical properties (similar n_2) to that of methanol. We find that decanol has greater spectral broadening potential than pentanol and preserves a Gaussian beam shape better than pentanol. We measure the M^2 value of our laser to be 1.38. After propagating through 1 cm of decanol, we measure an M^2 value of 1.51. The profiles of the beam with no decanol and after 1 cm of decanol can be seen in figures 4(a) and (b) respectively.

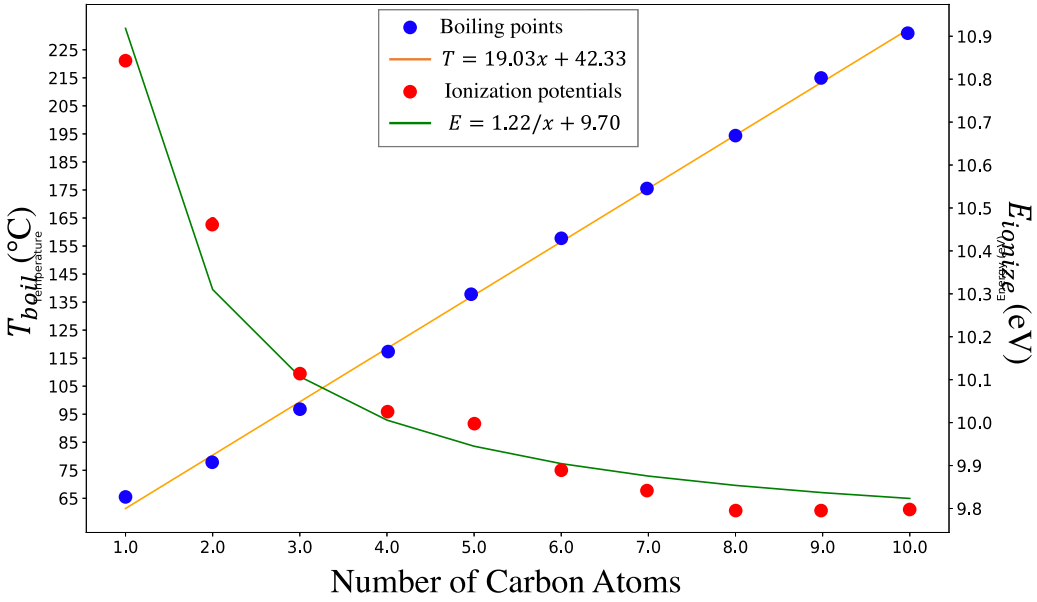

Figure 3. Boiling points and ionization potentials of alcohol chains as a function of the number of carbon atoms in the chain, e.g. 1.0 is methanol, 5.0 is pentanol, 10.0 is decanol. As the number of carbon atom in the alcohol chain increases, the boiling point increases linearly, while the ionization potential decreases as $\sim 1/x$. These two trends are indicative of the distortion of the beam shape being a product of thermal lensing, rather than plasma filamentation.

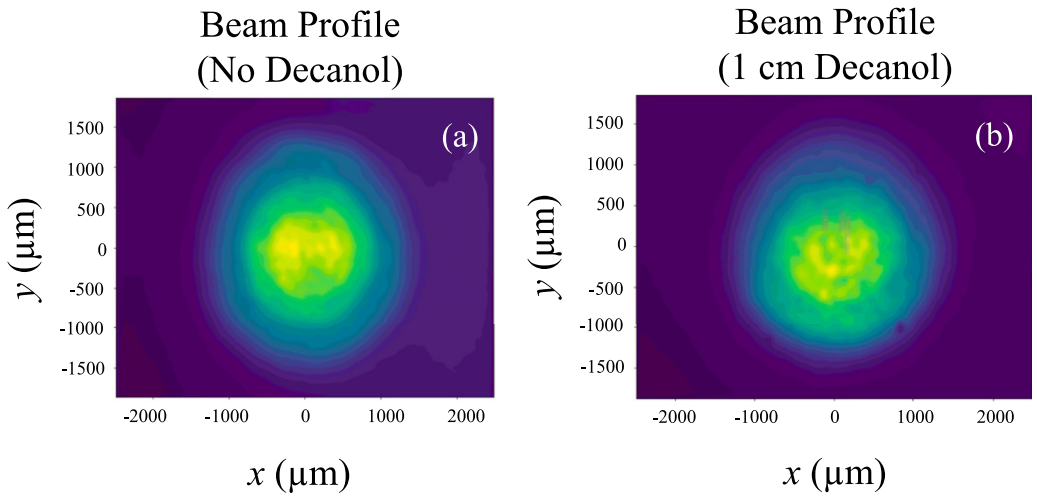

Figure 4. Gaussian beam profiles with (a) no decanol ($M^2 = 1.38$) and (b) 1 cm of decanol ($M^2 = 1.51$). The beam size was reduced by a factor of 2 to accommodate the dimensions of our camera (Thorlabs #CS165MU).

4. Pulse compression experiment

Using the previously mentioned Ti:sapphire laser, we are able to create a broad spectrum capable of supporting 42 fs pulses by passing the pulse through a 1 cm thick quartz cuvette filled with decanol. By passing the pulse through another 1 cm of decanol, we are able to generate a spectrum capable of supporting 25 fs pulses. We separate the cuvettes to reduce self-focusing, ensuring that we avoid damage to the material that would lead beam distortion. Figure 5(a) shows the spectrum of 1 cm of decanol (blue) and 2 cm of decanol (green) compared to the spectrum of our laser. The predicted bandwidth-limited pulses can be seen in figure 5(b); the colours of the pulse envelopes to the spectra of the same colour in figure 5(a).

After broadening the spectrum using 1 cm of decanol, we compress the pulse from 83.6 fs to 47.0 fs with a chirped mirror providing -1300 fs^2 of GDD (800 nm highly-dispersive ultrafast mirror from Edmund Optics #12–331). GDD is defined as $\mathrm{d}^2\phi/\mathrm{d}\omega^2$, the second derivative of the phase, ϕ, with respect to frequency, ω. GDD will cause the pulse to disperse as the group velocity is dependent on the frequency of the pulse; different frequency components will travel at different velocities. We pass the 47.0 fs pulse through another 1 cm of decanol, broadening the spectrum, followed by further compressing

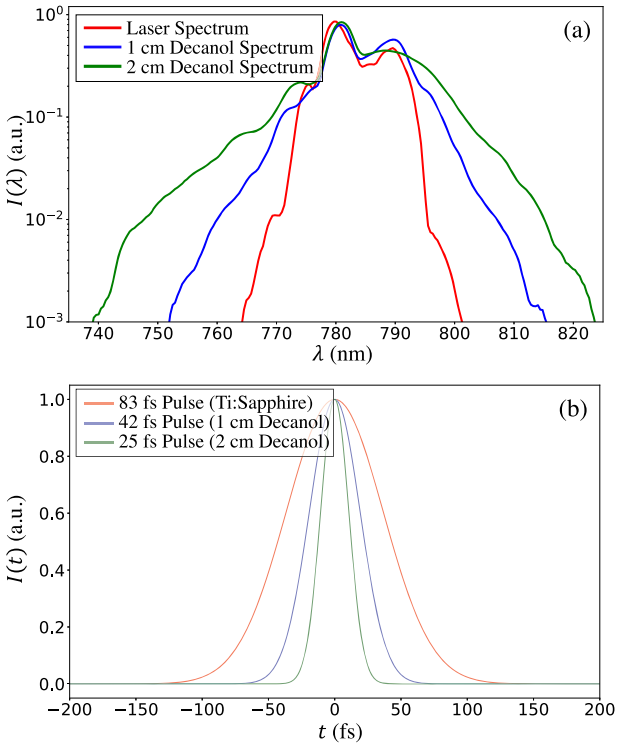

Figure 5. Shown in (a) are the spectra of the Ti:sapphire laser (dark red), 1 cm of decanol (dark blue), 2 cm of decanol (dark green). Shown in (b) are the bandwidth-limited pulses calculated from the spectra in (a). The spectra produced by the Ti:sapphire laser, 1 cm of decanol, and 2 cm of decanol support bandwidth-limited pulses of 83 fs (light red), 42 fs (light blue), and 25 fs (light green) respectively.

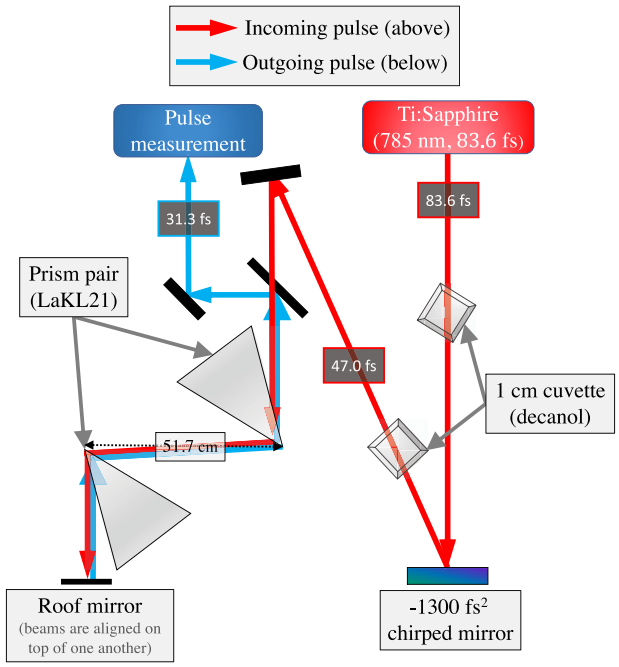

Figure 6. Sketch (top view) of the experimental setup used to compress the pulse twice using decanol. The pulse passes through a 1 cm cuvette filled with decanol and compresses after reflecting off a -1300 fs^2 chirped mirror. The pulse then passes through a second 1 cm cuvette filled with decanol and compresses a second time by passing through a LaKL21 prism pair. The pulse is then measured using a home-built pulse characterization apparatus. The pulse durations at each point in the experiment are shown in the shaded boxes. We measured a loss of 7.4% from the first cuvette of decanol and 7.1% from the second cuvette of decanol and a total loss of 36.4% including all other optics.

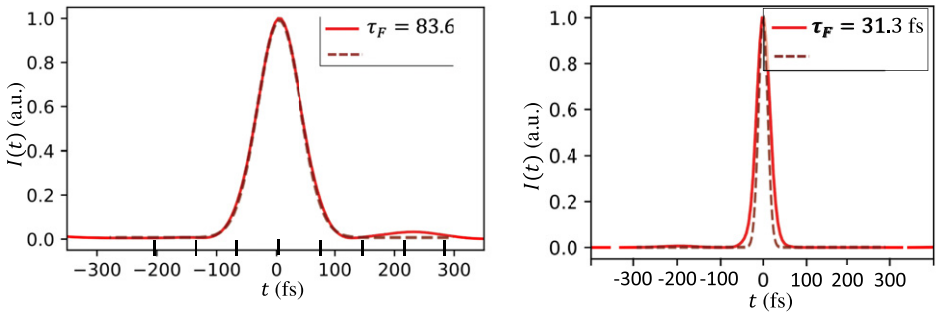

Figure 7. The pulses measured by FROG (τ_F) and their transform limit (τ_S). (a) 83.6 fs pulse produced by our Ti:sapphire laser (solid red) compared to the bandwidth-limited 83.6 fs pulse calculated from the spectrum of the Ti:sapphire laser (dashed maroon). (b) 31.3 fs pulse created via pulse compression using 2 cm of decanol (solid red) compared to the bandwidth-limited 25 fs pulse calculated from the spectrum of the 2 cm of decanol (dashed maroon). Using 2 cm of decanol, we were able to compress our pulse by a factor of 2.65.

the pulse from 47.0 fs to 31.3 fs using a LaKL21 prism pair (LaKL21 25.4 × 25.4 mm Ultrafast Prism from Edmund Optics #89–843) to provide tunable GDD. The prisms are placed 51.7 cm apart to achieve the ideal GDD needed to compress the pulse down to its bandwidth limit.

We pass the beam at its full size through the two cuvettes filled with decanol. Both cuvettes are placed at 31°, as close to Brewster's angle as possible given the dimensions of the cuvette and the beam diameter, to reduce the amount of back reflection off the surface of the cuvette. Reducing the back reflection allows for a more intense pulse to interact with the decanol, increasing the spectral bandwidth. A sketch of the experimental setup can be seen in figure 6. We measure a total power loss of 36.4%. We attribute 14.5% loss to the cuvettes of decanol (7.4% loss from the first cuvette, 7.1% loss from the second).

The pulses shown in figure 7 are characterized using a home built FROG. The pulse duration of our Ti:sapphire laser is measured to be 83.6 fs. After compressing the pulse, the pulse duration is reduced to 31.3 fs. We utilize an alternate compression factor: the ratio of the compressed pulse duration to the initial pulse duration. Our experiments yielded a total compression factor of 2.67 from 83.6 fs to 31.3 fs. After compressing the pulse twice, the beam shape retains a Gaussian intensity profile ($M^2 = 1.68$).

5. Conclusion

The goal of this work was to investigate the spectral broadening properties of alcohols as it pertains to pulse compression. In this study we investigate liquids as an alternative to solids and gases for pulse compression. We report the n_2 of 1-decanol to be $(6.8 \pm 0.5) \times 10^{-20}$ m^2 W^{-1}. We determined that decanol is capable of creating a broad spectrum capable of supporting sub-30 fs pulses. Using decanol, we generated a 31.3 fs pulse and measured it using FROG. We have shown decanol to be a good material to achieve 30 fs pulses as it is cheap, easy to use, and not susceptible to permanent damage. Decanol has proven to be a good complimentary material to hollow core gas-filled fibres and solid crystals. Using decanol, a laser with a longer pulse duration (80–100 fs) can be compressed down to 30–50 fs with ease, making any laser capable of performing experiments that require shorter pulse durations, such as IR or THz pulse generation [46, 47] and few-cycle pulse generation [48, 49]. Future studies will involve further compressing the pulse using additional passes through liquids, including alcohols.

Acknowledgments

We acknowledge funding support from the Natural Sciences and Engineering Research Council of Canada (NSERC) Discovery Grant Number RGPIN-2019-06877.

ORCID iDs

Jacob A Stephen https://orcid.org/0000-0001-6924-6883

References

[1] Hammond T J, Villeneuve D M and Corkum P B 2017 Producing and controlling half-cycle near-infrared electric-field transients *Optica* **4** 826–30
[2] Hammond T 2017 Spatio-temporal coupling to create sub-femtosecond pulses *J. Opt.* **19** 114002
[3] Vampa G *et al* 2018 Strong-field optoelectronics in solids *Nat. Photon.* **12** 465–8
[4] Vampa G, Hammond T J, Nesrallah M, Naumov A Y, Corkum P B and Brabec T 2018 Light amplification by seeded Kerr instability *Science* **359** 673–5
[5] Jayalath Arachchige C, Stephen J A and Hammond T J 2021 Amplification of femtosecond pulses based on $\chi^{(3)}$ nonlinear susceptibility in MgO *Opt. Lett.* **46** 5521–5
[6] Nie Z, Wu Y, Zhang C, Mori W B, Joshi C, Lu W, Pai C-H, Hua J and Wang J 2021 Ultra-short pulse generation from mid-IR to THz range using plasma wakes and relativistic ionization fronts *Phys. Plasmas* **28** 023106
[7] Hong Z, Rezvani S, Zhang Q and Lu P 2018 Ultrafast mid-IR laser pulses generation via chirp manipulated optical parametric amplification *Appl. Sci.* **8** 744
[8] Pires H, Baudisch M, Sanchez D, Hemmer M and Biegert J 2015 Ultrashort pulse generation in the mid-IR *Prog. Quantum Electron.* **43** 1–30
[9] Vampa G *et al* 2017 Plasmon-enhanced high-harmonic generation from silicon *Nat. Photon.* **11** 549–99
[10] Vampa G, Hammond T J, Thiré N, Schmidt B E, Légaré F, McDonald C R, Brabec T and Corkum P B 2015 Linking high harmonics from gases and solids *Nature* **522** 462–4
[11] Scutelnic V *et al* 2021 X-ray transient absorption reveals the ^{1}Au $(n\pi*)$ state of pyrazine in electronic relaxation *Nat. Commun.* **12** 5003
[12] Gaumnitz T, Jain A and Wörner H J 2018 Extreme-ultraviolet high-order harmonic generation from few-cycle annular beams *Opt. Lett.* **43** 4506–9
[13] Calegari F *et al* 2014 Ultrafast electron dynamics in phenylalanine initiated by attosecond pulses *Science* **346** 336–9
[14] Goulielmakis E *et al* 2004 Direct measurement of light waves *Science* **305** 1267–9
[15] Goulielmakis E, Yakovlev V S, Cavalieri A L, Uiberacker M, Pervak V, Apolonski A, Kienberger R, Kleineberg U and Krausz F 2007 Attosecond control and measurement: light-wave electronics *Science* **317** 769–75
[16] Cheng Y-C, Lu C-H, Lin Y-Y and Kung A H 2016 Supercontinuum generation in a multi-plate medium *Opt. Express* **24** 7224–31
[17] Vicentini E *et al* 2020 Nonlinear pulse compression to 22 fs at 156 μJ by an all-solid-state multipass approach *Opt. Express* **28** 4541–9
[18] Lu C-H, Tsou Y-J, Chen H-Y, Chen B-H, Cheng Y-C, Yang S-D, Chen M-C, Hsu C-C and Kung A H 2014 Generation of intense supercontinuum in condensed media *Optica* **1** 400–6
[19] He P *et al* 2017 High-efficiency supercontinuum generation in solid thin plates at 01 TW level *Opt. Lett.* **42** 474–7
[20] Silva F, Austin D R, Thai A, Baudisch M, Hemmer M, Faccio D, Couairon A and Biegert J 2012 Multi-octave supercontinuum generation from mid-infrared filamentation in a bulk crystal *Nat. Commun.* **3** 807
[21] Jeong Y-G *et al* 2018 Direct compression of 170 fs 50-cycle pulses down to 1.5 cycles with 70% transmission *Sci. Rep.* **8** 11794
[22] Haddad E *et al* 2018 Molecular gases for low energy pulse compression in hollow core fibers *Opt. Express* **26** 25426–36
[23] Köttig F, Tani F and Russell P S J 2020 Modulational-instability-free pulse compression in anti-resonant hollow-core photonic crystal fiber *Opt. Lett.* **45** 4044
[24] Safaei R, Fan G, Kwon O, Légaré K, Lassonde P, Schmidt B E, Ibrahim H and Légaré F 2020 High-energy multidimensional solitary states in hollow-core fibres *Nat. Photon.* **14** 733–9
[25] Beetar J E *et al* 2020 Multioctave supercontinuum generation and frequency conversion based on rotational nonlinearity *Sci. Adv.* **6** eabb5375
[26] Lötscher L and Vámos L 2015 Long-term stability of nonlinear pulse compression using solid-core large-mode-area fibers *J. Lasers Opt. Photon.* **02** 3
[27] Seidel M, Xiao X and Hartung A 2018 Solid-core fiber spectral broadening at its limits *IEEE J. Sel. Top. Quantum Electron.* **24** 2811907
[28] Schulte J, Sartorius T, Weitenberg J, Vernaleken A and Russbueldt P 2016 Nonlinear pulse compression in a multi-pass cell *Opt. Lett.* **41** 4511

[29] Viotti A-L, Seidel M, Escoto E, Rajhans S, Leemans W P, Hartl I and Heyl C M 2022 Multi-pass cells for post-compression of ultrashort laser pulses *Optica* **9** 197–216
[30] Krebs N, Pugliesi I and Riedle E 2013 Pulse compression of ultrashort UV pulses by self-phase modulation in bulk material *Appl. Sci.* **3** 153–67
[31] Hädrich S *et al* 2016 Energetic sub-2-cycle laser with 216 W average power *Opt. Lett.* **41** 4332–5
[32] Bozolan A, de Matos C J, Cordeiro C M B, dos Santos E M and Travers J 2008 Supercontinuum generation in a water-core photonic crystal fiber *Opt. Express* **16** 9671
[33] Sheik-Bahae M, Said A A, Wei T-H, Hagan D J and Van Stryland E W 1990 Sensitive measurement of optical nonlinearities using a single beam *IEEE J. Quantum Electron.* **26** 760–9
[34] Stryland E W V and Sheik-Bahae M 1997 Z-scan technique for nonlinear materials characterization *Materials Characterization and Optical Probe Techniques: A Critical Review* vol 10291 ed R A Lessard and H Franke (Bellingham, Washington: International Society for Optics and Photonics, SPIE) pp 488–511
[35] Nibbering E T J, Franco M A, Prade B S, Grillon G, Le Blanc C and Mysyrowicz A 1995 Measurement of the nonlinear refractive index of transparent materials by spectral analysis after nonlinear propagation *Opt. Commun.* **119** 479–84
[36] Major A, Yoshino F, Nikolakakos I, Aitchison J S and Smith P W E 2004 Dispersion of the nonlinear refractive index in sapphire *Opt. Lett.* **29** 602–4
[37] Ho P P and Alfano R R 1978 Optical Kerr effect in liquids *Phys. Rev.* A **20** 2170–87
[38] Chin S L *et al* 2012 Advances in intense femtosecond laser filamentation in air *Laser Phys.* **22** 1–53
[39] Li Y-C, Kuo S-Z, Wei T-H, Wang J-N, Yang S S and Tang J-L 2009 Control of thermal lensing effect in transparent liquids by femtosecond laser pulses *Japan J. Appl. Phys.* **48** 09LF06
[40] Dobek K 2022 Thermal lensing: outside of the lasing medium *Appl. Phys.* B **128** 18
[41] Ortega J 1982 Densities and refractive indices of pure alcohols as a function of temperature *J. Chem. Eng. Data* **27** 312–7
[42] O'Neil M 2001 *The Merck Index–An Encyclopedia of Chemicals, Drugs, and Biologicals* 13th edn (Rahway, New Jersey: Merck and Co., Inc.)
[43] Strycker B D *et al* 2012 Energy transfer between laser filaments in liquid methanol *Opt. Lett.* **37** 16–8
[44] Qi P, Lin L, Su Q, Zhang N, Sun L and Liu W 2017 *In situ* visualization of multiple filament competition dynamic during nonlinear propagation of femtosecond laser *Sci. Rep.* **7** 10384
[45] Haynes W 2015 *CRC Handbook of Chemistry and Physics* 95th edn (Boca Raton, FL: CRC Press)
[46] Clerici M *et al* 2013 Wavelength scaling of terahertz generation by gas ionization *Phys. Rev. Lett.* **110** 253901
[47] Fan H-T, Xu C-H, Wang Z-H, Wang G, Liu C-J, Liang J-K, Chen X-L and Wei Z-Y 2014 Generation of broadband 17 μJ mid-infrared femtosecond pulses at 375 μm by silicon carbide crystal *Opt. Lett.* **39** 6249–52
[48] Liang H *et al* 2017 High-energy mid-infrared sub-cycle pulse synthesis from a parametric amplifier *Nat. Commun.* **8** 141
[49] Carlson D R, Hutchison P, Hickstein D D and Papp S B 2019 Generating few-cycle pulses with integrated nonlinear photonics *Opt. Express* **27** 37374–82